p53 R175H Hydrophobic Patch and H-Bond Reorganization Observed by MD Simulation

Kelly M. Thayer,[1,2] Taylor R. Quinn[1,3]

[1] *Department of Chemistry, Vassar College, 124 Raymond Ave, Poughkeepsie, NY, 12604*

[2] *Department of Chemistry, Hall-Atwater Laboratories, Wesleyan University, Middletown, CT, 06459*

[3] *Department of Chemistry, University of Notre Dame, Notre Dame, IN, 46556*

Received 27 July 2015; revised 6 November 2015; accepted 10 November 2015
Published online 13 November 2015 in Wiley Online Library (wileyonlinelibrary.com). DOI 10.1002/bip.22766

ABSTRACT:

Molecular dynamics simulations probe the origins of aberrant functionality of R175H p53, which normally prevent tumorigenesis. This hotspot mutation exhibits loss of its essential zinc cofactor, aggregation, and activation of gain of function promoters, characteristics contributing to the loss of normal p53 activity. This study provided molecular level insight into the reorganization of the hydrogen bonding network and the formation of a hydrophobic patch on the surface of the protein. The hydrogen bonding network globally redistributes at the expense of the stability of the β-sandwich structure, and surface residues reorganize to expose a 250 Å^2 hydrophobic patch of residues covering approximately 2% of the solvent accessible surface. These changes could both stabilize the protein in the conformation exposing the patch to solvent to mediate the reported aggregation, and cause a destabilization in the area associated with DNA binding residues to affect the specificity. The development of the patch prior to loss of zinc indicates that stabilizing the patch quickly may prevent zinc loss. Considerations for rational design of small molecule therapeutics in light of the structural insight has been discussed and it suggest the positive ring around the hydrophobic patch and conserved residues may constitute a druggable site. © 2015 Wiley Periodicals, Inc. *Biopolymers 105: 176–185, 2016.*

Keywords: molecular dynamics; p53; cancer; rational drug design

This article was originally published online as an accepted preprint. The "Published Online" date corresponds to the preprint version. You can request a copy of any preprints from the past two calendar years by emailing the Biopolymers editorial office at biopolymers@wiley.com.

INTRODUCTION

The protein p53 asserts a vital role in preventing cancer; some 50% of all human cancers involve mutant p53.[1] Often termed the "guardian" of the genome,[2] the protein carries out two vital processes: prior to DNA replication, it signals for DNA repair should DNA damage be present, and when DNA sustains damage beyond repair, it signals for apoptosis to eradicate defunct cells.[3–6] Mouse knockout models have shown that when this guardian itself becomes incapacitated, the lack of a check system allowed growth of tumors.[7–9]

Dubbed one of the "hotspots" in p53,[10] R175H is one of the most oncogenic mutations in the protein,[11] exhibiting several aberrant phenotypes. Numbering among mutations that not only lack typical transcription activity, it also introduces gain of function mutations, allowing it to activate promoters not normally under its control to further contributing to tumorigenesis.[11–16] R175H mutants exhibit abolished activity in responding to double strand DNA breakage and the ability to induce interchromosomal translocation rearrangements that introduce a high level of genetic instability,[11] contributing to

Correspondence to: Kelly M. Thayer; e-mail: kthayer@wesleyan.edu
Contract grant sponsors: Elise Nichols and Margaret Sawyer Bloch Chemistry Research Fellowship (TRQ)

the aggressive nature of this mutation. That it is found associated with the heat shock protein hsp70, a folding chaperone protein, suggests that it is at least partially unfolded.[17] Similarly, early studies involving the development of antibodies which differentiate between folded and unfolded p53 point toward an unfolded R175H mutant.[18,19]

The R175H mutant has furthermore been associated with the loss of the tetrahedrally coordinated zinc ion which also leads to structural instability.[20,21] A series of chelation experiments have established p53 as a zinc dependent metalloprotein.[21] Bridging two loops of the protein, the Zn^{2+} globally stabilizes the protein and helps orient the loop L3 for binding to DNA in the minor groove, and thus its loss is associated with lower stability.[22] The protein, even when bound to zinc, exhibits relatively low stability, having a melting temperature of 45°C.[23] As a result, even small perturbations can lead to partial unfolding and aggregation.[24] While wild type p53 binds one Zn^{2+} per domain stably at 20°C for several days[25] with a dissociation rate on the order of 1×10^{-6} at 10°C,[26] the R175H mutated protein donates its zinc to chelators within minutes.[27] The folding process of p53 is fairly complex, with six reported intermediates, and proteins with a loss of zinc appear to have more rapid exchange between folded and unfolded states,[25,28] leading to hydrophobic aggregation within minutes at physiological temperature.[27]

The complete 393 amino acid sequence of p53[29,30] contains three domains: the transactivation domain, the DNA binding domain (DBD) containing the sequence specific DNA binding functionality, and the COOH-terminal domain involved in tetramerization.[21] While the full length sequence has eluded structure determination in atomistic detail, the vast majority of the tumorigenic mutations including R175H map to the core domain[31] which has been crystallized.[22,32] Overall, the DBD assumes a classic β-sandwich configuration of antiparallel β-sheets held together by interstrand H-bonding. The structure has identified several key features of the p53 protein (Figure 1), among them four loops involved in the recognition of the binding site termed loops L1 to L3 and strand loop helix, as well as a chelated zinc tetrahedrally coordinated by cys176 and his179 in loop 2, and cys238 and cys242 in loop 3.[22] Tethering of the second and third loop at the coordination site likely plays a role in positioning them for proper interaction with the DNA, conferring the transcription factor functionality. Eight residues make direct hydrogen bonds with the DNA in the crystal structure, mediating the protein–DNA interaction.

Structural determination and molecular dynamics has facilitated a molecular understanding of the workings of tumorigenic mutations and guided rational drug design in hopes of restoring wild type activity in hotspot mutations.[33–36] Recently, the mutations R249S and T123A and their restoration by H168R both individually and as double and triple mutants have been explored,[37] as have the interactions of p53 with DNA in the R273H/C mutants.[38] Focusing on the Y220C

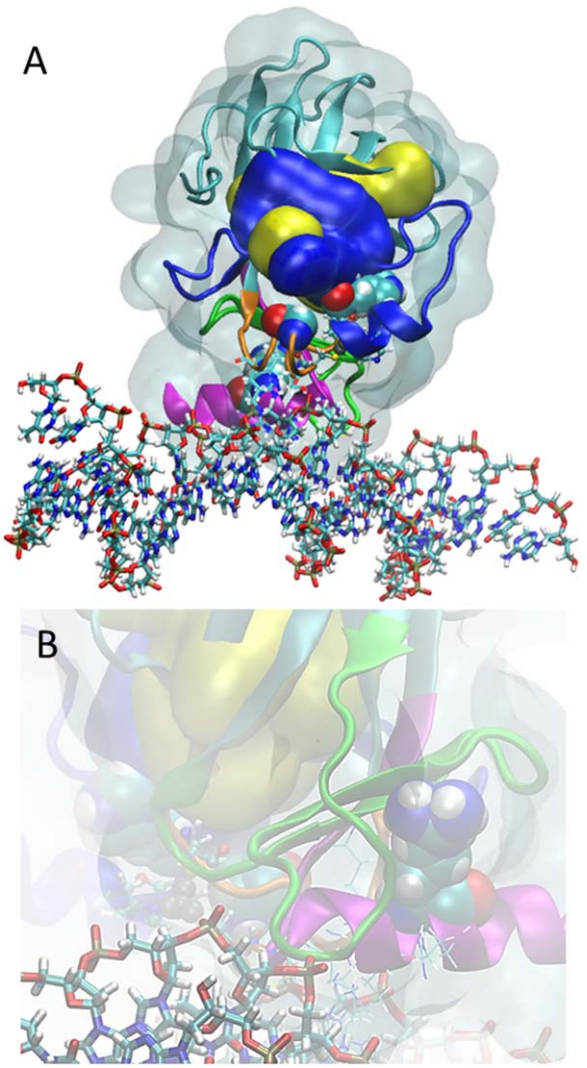

FIGURE 1 Hydrophobic pocket in relation to key features of p53. Features are mapped to an MD snapshot of the R175H_1 simulation in which the pocket has grown in. The views are (**A**) pocket side and (**B**) zoomed on zinc. Features are displayed as follows: protein surface in *transparent cyan*, protein backbone in *cyan cartoon* with loops colored, loop L1 residues 113–140 *green*, loop L2 residues 163–195 *royal blue*, loop L3 residues 236–251 *orange*, strand loop helix residues 271–286 *magenta*; hydrophobic pocket residues A156, M160, A161, V172, V173, L194, I195, V216, Y234 shown as *yellow surface*, positive ring R174, H193, R213, H214 shown as *blue surface*; *zinc grey* VDW, zinc coordination residues C176, H179, C238, C242 in CPK by element colors as *ball* and *stick*; residues hydrogen bonding with DNA K120 R241 R248 K273 A276 A277, R280 R283 in *sticks*; DNA in CPK colors by element as *thick sticks*. R175H mutation as VDW in *CPK colors*.

mutant, two novel compounds, PK083[39] and PK7088[40] operate by substituting for the lost aromatic side chain, thereby restoring structural stability to the protein.

At present, small molecule therapeutics effective for R175H are eagerly sought. The R175H mutation has been targeted by the compound NSC319726 (also referred to as zinc metallochaperone-1 [ZMC1]) which restores function by increasing cellular concentrations of zinc, facilitating the stability of p53.[41] PRIMA-1 and its analog PRIMA-1^{MET} (APR46), metabolically converted to methylene quinuclidinone, which is capable of forming adducts with cysteine thiols, hold promise for this mutant as well.[42] Treatment with this small molecule has shown up regulation of Bax, Puma, and Nox, three target p53 genes used as markers to indicate restoration of normal function,[43] and has advanced to clinical trials.[44] Recent molecular dynamics simulations of the R175H mutation have investigated the opening of a pocket located between L1 loop and sheet S3 centered about cys124, whose mutation abolishes reactivation by PRIMA-1.[45] Further understanding of R175H mutant dynamics holds potential to expand the arsenal of R175H therapeutics to include rationally designed small molecules acting with specificity to this p53 mutation. Specific treatments are of value because off-target side effects remain a formidable barrier for promising therapeutics to advance through clinical trials.[3]

In this study, we have endeavored to examine the dynamic structural nature of the R175H hotspot mutation. Molecular dynamics (MD) simulations[46] provide structural and energetic information on macromolecules at the atomistic level consistent with experiment with detailed information regarding the time evolution of conformations, including those which have evaded structural determination. This methodology has been implemented to examine the dynamics of the 1TUP wild type crystal structure and the R175H engineered mutant counterpart, revealing the emergence of a hydrophobic patch in the mutant structure and the structural reorganization which characterizes the mutation. We offer a mechanistic molecular level explanation of the aberrant phenotypic characteristics of the R175H mutant protein and suggest, with this molecular resolution vantage, the pocket and surrounding residues as a possible druggable site targetable with rational drug design that may restore wild type functionality.

RESULTS

Observation of Development of Hydrophobic Patch in R175H Mutant Simulation

In order to characterize differences between the wild type p53 DBD and the corresponding R175H mutant, stable simulations with RMSD fluctuations centering around 3.5 Å were obtained and compared. The simulations are 1TUP_wt, the unmutated DBD bound to DNA as found in the 1TUP crystal structure, and R175H_1, the same system with the mutation introduced. Interestingly, the opening up of a hydrophobic patch on the surface of the mutant was observed on the surface of the protein distal from the mutation directly adjacent to the zinc chelation site (Figure 1). The opening of the pocket to expose the patch revealed itself within the first five nanoseconds of the total simulation, and consisted of the residues A159, M160, A161, V172, V173, L194, I195, V216, and Y234. A ring of basic residues, consisting of R174, H193, R213, and H214 encircles the hydrophobic patch. To verify this result, an independent MD simulation of the mutant, R175H_2, was carried out, and the formation of the patch was again observed within the first 5 ns of the simulation.

Quantitation of Patch Size

To quantitatively assess the size of the patch, the time evolution of the solvent accessible surface area of the patch was followed over the course of 15 ns for the wild type and mutant, as well as for R175H_2, the replicate. Figure 2 shows the solvent accessible surface area of the hydrophobic patch residues and total protein surface area for the two replicates as compared with the wild type simulation. The surface area of the patch residues stabilizes at about 200 Å^2 in the wild type (panel A), with an increase around the fourth nanosecond which quickly dissipates. The mutants begin with a higher exposure around 250 Å^2; since the mutant was engineered off the wild type crystal structure, the difference had already appeared during equilibration. The surface area of the mutant replicates stabilizes at about 250 Å^2, which is about 50 Å^2 higher than the wild type. The overall surface area of the mutant protein (panel B) also is higher than that of the wild type.

Reorganization of the H-Bond Network

In order to gain insight into these structural changes, the hydrogen bonding network was investigated for the 1TUP_wt and R175H_1 and R175H_2 simulations over the first five nanoseconds of the simulations, the time frame in which the patch developed and stabilized. Hydrogen bonds found within any of the structures were monitored in all structures and are reported in Table I. The crystal structure 1TUP contains the fewest hydrogen bonds, and the R175H mutant loses H-bonds after the development of the patch. The 1TUP_wt likewise loses H-bonds from the end of equilibration to the end of dynamics, but it maintains more than either of the mutants. This is consistent with the greater stability of the wild type protein. About 15 H-bonds possessed by the 1TUP_wt at the 5 ns

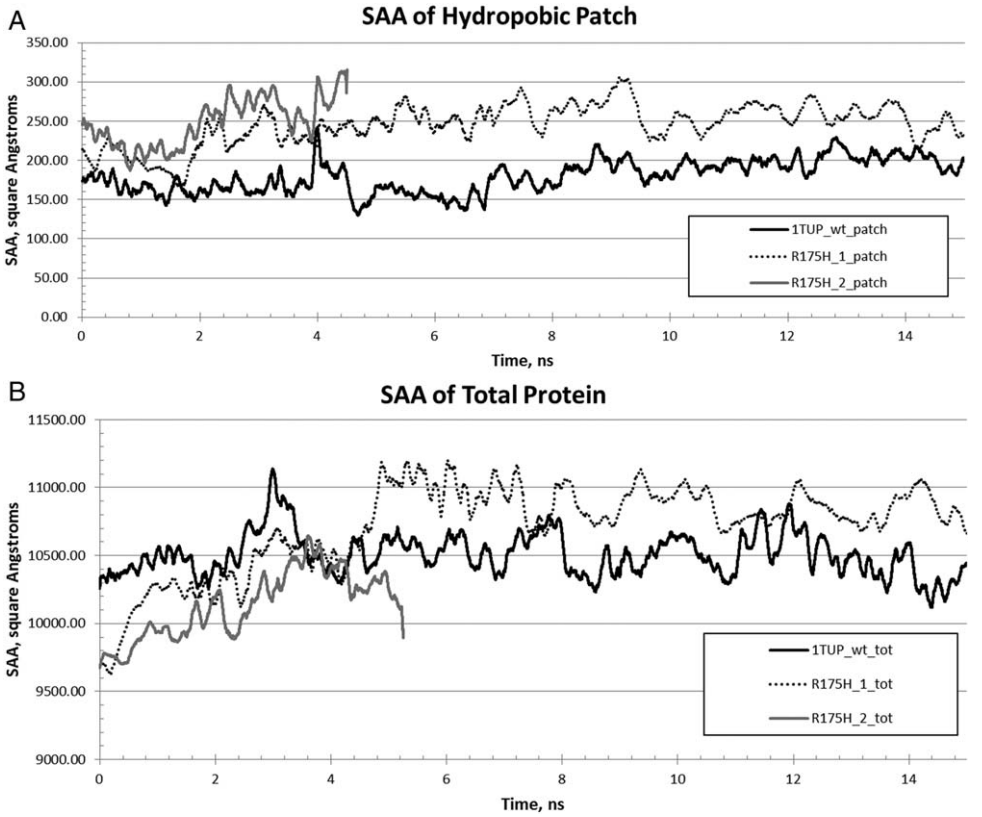

FIGURE 2 Solvent accessible surface area of patch and whole protein. SAA of (**A**) patch residues and (**B**) entire protein surface for the three simulations as a function of simulation time in nanoseconds.

mark are lost by both copies of the mutants, and an additional 16 are lost for either of the two replicates. To compensate for the loss, both mutants make five of the same new contacts, and copy 1 gains 18 new contacts and copy 2 gains 19. In this view, the 1TUP_wt contains a total of 37 H-bonds, an intermediate value between 42 total for R175H_1 and 33 for R175H_2. Thus the number of bonds itself unlikely confers the difference in stability between the mutant and wild type, prompting an examination of the location of the hydrogen bonds as a possible explanation for the differences in stability.

Assessment by comparing which hydrogen bonds were present at the 5 ns snapshots of the simulations of the structural mapping of the hydrogen bonds indicated a global reorganization involving all but 6 hydrogen bonding pairs out of the 79 possessed among the 5 ns simulations (Table I). Figure 3 details the changes occurring in the hydrogen bonding network, and the number of H-bonds lost and gained between the structural elements were tabulated (Table II). Examination of the net number of H-bonds between structural elements indicates that both simulation copies of the R175H resulted in loss of 4 and 10 hydrogen bonds at 5 ns as compared with the wild type, indicating that when the hydrophobic patch emerges, the hydrogen bonding network between structural elements diminishes, while the new hydrogen bonds which are formed either counterbalance those which were lost or form outside secondary structural elements. Furthermore, both mutants lose the hydrogen bond to H175, the site of the mutation.

DISCUSSION

Having reported a molecular level description of the structural reorganization occurring in p53 R175H mutation, we discuss possible mechanisms by which the R175H mutation may acquire its especially carcinogenic phenotypes and the implications for the development of small molecule therapeutics. The examination of R175H simulations in replicate associated with zinc binding as compared with the wild type and the observance of a quickly opening pocket of hydrophobic residues in the core to display a hydrophobic patch within the first nanosecond of R175H suggests a role for H-bond rearrangement and provides insight into possible rational design strategies that may stabilize R175H mutant p53.

Table I Hydrogen Bond Assessment

Index	Resid #		1TUP xtal	1TUP		R175H_1		R175H_2
	DON	ACC	(NA)	0 ns	5 ns	0 ns	5 ns	5 ns
1	96	211	0	0	0	0	0	1
2	100	98	0	0	1	0	0	0
3	104	110	1	0	0	0	0	0
4	110	108	1	1	0	1	0	0
5	110	146	0	0	0	0	0	1
6	110	146	0	1	0	1	0	0
7	116	124	0	0	1	0	0	0
8	122	119	0	1	0	1	0	1
9	125	117	0	1	0	1	0	0
10	125	134	0	0	1	0	1	1
11	126	131	0	0	0	0	1	0
12	127	132	0	1	1	1	1	1
13	127	286	0	0	1	0	0	1
14	132	285	0	1	1	1	0	0
15	133	271	1	1	1	1	1	1
16	134	125	0	1	1	1	0	0
17	136	123	0	0	0	0	1	0
18	138	236	0	1	0	1	0	0
19	140	198	0	0	0	0	0	1
20	141	234	0	1	1	1	0	0
21	143	232	0	1	1	0	1	1
22	144	112	1	0	1	0	1	0
23	145	230	0	0	0	0	0	1
24	146	110	0	1	0	1	0	0
25	148	107	0	0	0	0	1	0
26	155	158	0	0	0	0	0	1
27	157	218	0	1	0	1	1	0
28	158	256	0	1	1	1	1	0
29	158	258	0	1	1	1	1	1
30	158	258	0	0	0	1	0	1
31	159	216	0	1	1	1	1	0
32	162	252	0	0	0	0	0	1
33	164	250	1	1	0	1	0	0
34	164	271	0	0	0	0	1	0
35	169	165	0	0	0	0	0	1
36	171	168	0	0	0	0	1	1
37	175	192	0	0	1	0	0	0
38	180	176	0	0	0	0	1	0
39	181	177	0	1	0	1	0	0
40	182	178	1	1	0	1	0	0
41	183	179	0	0	0	0	1	0
42	183	180	0	0	1	0	0	1
43	185	184	0	0	0	0	1	0
44	185	189	1	0	0	0	0	0
45	189	186	1	1	0	1	0	0
46	192	192	0	1	0	1	0	0
47	196	235	1	0	0	0	1	1
48	198	233	0	1	1	1	0	0
49	204	217	0	1	1	1	0	0
50	206	215	1	1	1	1	1	0
51	208	213	1	0	0	0	0	0
52	209	258	0	0	1	0	0	0
53	211	208	0	0	1	0	1	0

Table I *Continued*

Index	Resid # DON	Resid # ACC	1TUP xtal (NA)	1TUP 0 ns	1TUP 5 ns	R175H_1 0 ns	R175H_1 5 ns	R175H_2 5 ns
54	212	208	0	1	0	1	0	0
55	213	161	0	0	0	0	1	0
56	213	171	0	0	1	0	1	1
57	215	206	0	0	0	0	1	0
58	216	159	0	0	0	0	1	1
59	217	204	0	1	0	1	0	1
60	218	157	1	1	0	1	0	0
61	227	224	0	0	0	0	1	0
62	230	221	0	0	0	0	0	1
63	232	143	0	1	1	1	0	0
64	235	140	0	0	0	0	1	0
65	235	198	0	1	0	1	0	1
66	237	194	1	1	0	1	0	0
67	240	274	1	0	1	0	1	0
68	241	239	0	0	0	0	1	0
69	249	171	1	1	1	1	1	0
70	249	171	0	1	0	1	1	1
71	249	245	0	1	0	1	0	0
72	249	246	1	0	0	0	1	0
73	251	252	0	0	0	0	0	1
74	251	272	0	0	0	0	0	1
75	252	162	0	1	1	1	1	0
76	253	270	1	1	1	1	0	0
77	254	160	1	1	1	1	0	0
78	256	158	0	1	0	0	1	1
79	257	266	0	1	0	1	1	0
80	258	156	0	1	1	1	1	0
81	259	261	0	0	1	0	0	0
82	259	263	0	0	0	0	1	0
83	260	259	1	1	0	1	0	0
84	261	259	0	0	0	0	0	1
85	262	259	0	0	0	0	1	0
86	265	257	0	1	0	1	0	0
87	267	101	0	0	0	0	0	1
88	267	103	1	1	0	1	0	0
89	268	267	0	0	0	0	0	1
90	268	255	0	0	1	0	0	0
91	269	100	0	0	1	0	0	1
92	271	131	0	0	1	0	1	0
93	272	251	0	1	1	1	1	0
94	273	133	0	1	0	1	0	0
95	275	135	1	1	1	1	0	0
96	280	281	0	1	0	1	0	0
97	281	277	0	0	0	0	1	0
98	282	278	0	0	1	0	1	0
99	282	286	0	0	1	0	1	0
100	283	287	0	0	0	0	0	1
101	284	280	0	1	0	1	0	0
102	286	282	0	0	0	0	0	1
Total H-bonds:			21	47	37	46	42	33

The presence (1) or absence (0) of hydrogen bonds between donor (DON) and acceptor (ACC) residues was assessed for the 1TUP crystal structure (Ref. 22) and the three simulations of this study at the end of equilibration and at 5 ns. Note that the R175H_1 0 ns results serve as the reference state for both mutant replicates because the H-bond pattern was observed to be the same for both at that point. Total hydrogen bond counts appear at the bottom of the respective columns.

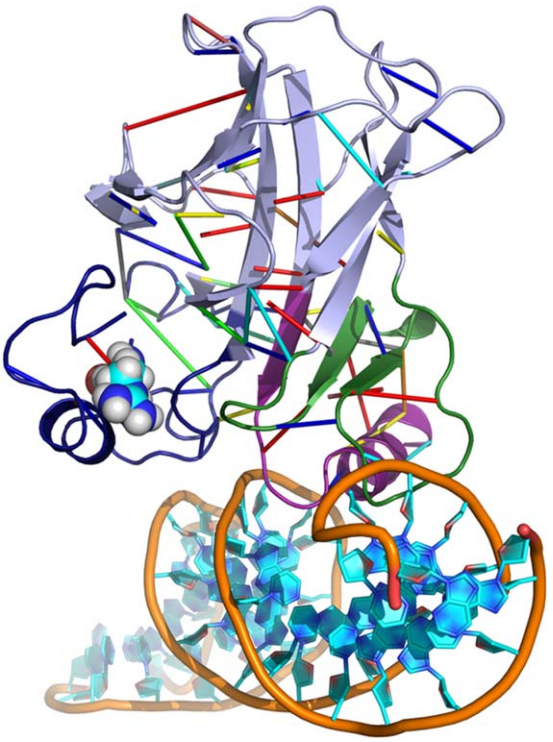

FIGURE 3 H-bond network exchange. The H-bonds lost and gained by the 5th ns of simulation are depicted with respect to p53 key features (*colors* as in Figure 1) and the mutation site in VDW. All lost and gained H-bonds are displayed as lines between alpha carbons of residues and are colored as follows: H-bonds lost by R175H simulations: both R175H simulations (*red*), R175H_1 (*orange*), R175H_2 (*yellow*); H-bonds gained by both R175H simulations: both R175H simulations (*green*), R175H_1 (*cyan*), R175H_2 (*purple*).

The development of a hydrophobic pocket within the first nanosecond and stabilization throughout 15 ns of simulation time suggests that this patch may be a site of hydrophobic aggregation between p53 proteins, consistent with reports of aggregation.[27] Given that p53 is a relatively unstable protein as evidenced by its low melting temperature,[23] that a single point mutation is sufficient to perturb the free energy surface sufficiently to effect unfolding would likely require a free energy difference on the order of a few kcal/mol, rendering this a plausible event. Binding to gain of function promoters could occur while the protein is in this destabilized state prior to undergoing aggregation and loss of zinc. Thus, a small molecule may be able to prevent such activity by patching over the hydrophobic area, similar to the approach taken for the development of PK083[39] and PK7088[40] which operate by filling the void created by the Y220C mutation.

An interesting question is whether the zinc is lost before or after the development of the hydrophobic pocket. The simulations presented here suggest that for the case of R175H, the pocket formation precedes the loss of zinc, since the pocket formation was observed, but the zinc remained intact for the full duration of the simulation. That R175H appears to rapidly display the hydrophobic residues prior to loss of zinc lends itself to the idea that discovery of a therapeutic to prevent partially unfolded proteins from aggregating with the pocket as a nucleation site could possibly prevent the loss of the zinc as well. Given that the requisite zinc, which provides structural scaffolding between loops L2 and L3 (Figure 1), is necessary for proper function and that this mutation in particular

Table II Hydrogen Bonding Between Structural Elements

	H-Bonds Lost			H-Bonds Gained			Net	
Structural Element	Both	R175H_1 Exclusively	R175H_2 Exclusively	Both	R175H_1 Exclusively	R175H_2 Exclusively	R175H_1	R175H_2
S1–S3	0	0	1	0	0	1	0	0
S2–S2′	1	0	0	0	0	0	−1	−1
S3–S8	2	0	0	0	0	1	−2	−1
S8–S5	1	0	0	1	0	0	0	0
S6–S7	1	0	1	0	1	0	0	−2
S7–S4	0	0	1	1	0	0	1	0
S4–S9	1	0	3	1	0	1	0	−2
S9–S10	2	0	1	0	1	1	−1	−2
H2–S2	0	0	0	0	0	0	0	0
H2–S2′	1	0	1	0	0	0	−1	−2
Total	**9**	**0**	**8**	**3**	**2**	**4**	**−4**	**−10**

The number of hydrogen bonds lost and gained between secondary structural elements in p53 mutant simulations R175H_1 and R175H_2 as compared with the wild type simulation, all at the 5th ns, are tabulated from the interactions depicted in Figure 3 Panels A–C. Structural elements beginning with S indicate β-strands and those with H indicate helices, numbered as indicated in the schematic (Figure 3 Panel C).

involves gain of function implying that the specificity of the active site becomes altered, stabilization of zinc is likely to be an essential aspect of restoring native p53 functionality, and preventing aggregation may be insufficient to restore native function. Thus, adding back the zinc may also need to be addressed. Loh et al. have recently reported on the ZMC1 that operates by locally increasing the concentration of zinc to restore function.[41,47] However, how a generalized increase in zinc concentration in the cell may affect zinc binding to non-native or low affinity sites in other proteins will likely be topics of investigation as this idea becomes developed. If it is true that zinc loss promotes partial unfolding in some cases, the generalized approach of increasing zinc concentration would possibly be more effective, whereas if the patch development occurs first in some mutants, as appears to be the case with R175H, the use of a specific small molecule therapeutics to restore native function could be the strategy of choice due to greater specificity and fewer cross-reactions with other zinc metalloproteins.

This exemplifies how individualized medicine based on the sequence of a patient's particular p53 variant could be utilized to tailor a treatment approach. A key advantage to the development of mutation specific therapies is the promise of mitigating both on-target and off target side effects, which continue to hinder promising small molecules as they pass through clinical trials.[3] In light of this, this present study sheds light on how a small molecule may be designed to both stabilize the R175H mutant, possibly in the native conformation, to prevent unfolding and stabilize the zinc binding.

Speculating as to the druggability of the patch, Figure 4 shows the patch exposed in the R175H mutant along with the ring of positively charged residues encircling it, offering a number of potential hydrogen bond donor and acceptor sites. An effective therapeutic in its role of preventing aggregation would cover over the hydrophobic residues and could gain specificity by interacting with these charged residues. Furthermore, therapeutics able to resist escape mutations will likely result in more robust clinical treatments.[48,49] We have developed a computational screen to estimate the relative free energy of mutation of all possible point mutants and have reported this for the MDM2-p53 N-terminal tail interaction (Thayer, K.M. and Beyer, G.A., MS, in prep), which argues that energetically constrained residues are desirable contact points for small molecule therapeutics because their mutation energetically destabilizes the protein and thus such mutants are likely to be removed from the gene pool due to selection pressure.[50] We have also carried out such calculations for p53 1TUP wild type structure (Thayer, K.M., Beyer, G.A., and Kugelmass, L., MS, in prep) and in the wild type structure, Glu171, Asn247, and Arg249 are energetically constrained residues near the patch, suggesting these would be primary sites of interest to target.

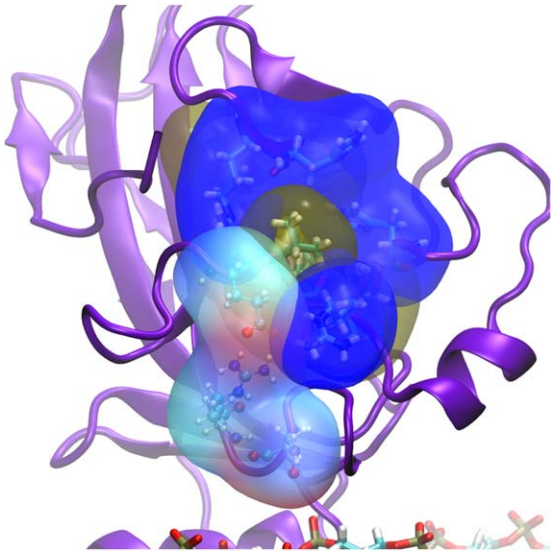

FIGURE 4 Druggability of the hydrophobic patch. hydrophobic patch (*yellow transparent surface, enclosed sticks*), positively charged ring (*blue transparent surface, enclosed sticks*), and energetically constrained residues near the patch (*CPK colored transparent surface, CPK colored ball and sticks*) show an area on the surface of R175H mutant p53 that could possibly serve as a target site for rational drug design.

We have presented herein a molecular dynamics study of the R175H mutant of p53 and report the observation of the rapid development of a hydrophobic patch encircled by positively charged residues. We suggest that this patch could serve as a nucleation site for hydrophobic aggregation, and thus a small molecule covering the patch may be able to prevent aggregation and possibly loss of zinc in hopes of restoring native anti-tumor functionality. We have presented some suggestions that may be useful for the rational design of a therapeutic small molecule targeting this pocket that may be restorative of native function, which may pave the way to the development and implementation of novel clinical treatments to counter the R175H hotspot mutation.

MATERIALS AND METHODS

Study of the p53 protein was conducted on the DNA-binding domain using the crystal structure 1TUP[22] as the starting structure, using the chain B DBD monomer bound to a consensus DNA binding site. Molecular dynamics simulations were carried out using the Parm99[51] force field and Amber12 suite of programs.[52,53] Zinc was modeled using the cationic dummy atom approach[54,55] utilizing the parameters provided from the Mayo Clinic Pang lab web site http://www.mayo.edu/research/labs/computer-aided-molecular-design/projects/zinc-protein-simulations-using-cationic-dummy-atom-cada-approach. In truncated octahedral boxes, the systems were fully solvated with

explicit TIP3P[56] water with a minimum distance of 10 Å from the box and counterions to electroneutrality. About 15 ns thermocoupled 298 K simulations were carried out on wild type p53, and the mutation R175H was engineered into the crystal structure as a point mutation using the tleap module of Amber12. A replicate of R175H was set up and run by reassigning velocities to the same starting structure such that the trajectory is unique from the first replicate, with collection of 5 ns of production data, the time over which the patch arose in the first replicate. Trajectories were analyzed using cpptraj.[57] Results were visualized using VMD[58] and PyMol.[59] Hydrogen bond analysis was carried out using VMD[58] with a heavy atom cutoff of 3.0 Å and an angle cutoff of 20 degrees.

The authors gratefully acknowledge Mark Smith and Stephen M. Beare for technical assistance and access to Center for Collaborative Approach to Science computer resources at Vassar College. The authors wish to thank D. L. Beveridge for a critical reading of the manuscript. The authors declare that they do not have any conflicts of interest.

REFERENCES

1. Vogelstein, B.; Lane, D.; Levine, A. J. Nature 2000, 408, 307–310.
2. Lane, D. P. Nature 1992, 358, 15–16.
3. Khoo, K. H.; Hoe, K. K.; Verma, C. S.; Lane, D. P. Nat Rev Drug Discov 2014, 13, 217–236.
4. Speidel, D. Arch Toxicol 2015, 501–517.
5. Wasylyk, C.; Salvi, R.; Argentini, M.; Dureuil, C.; Delumeau, I.; Abecassis, J.; Debussche, L.; Wasylyk, B. Oncogene 1999, 18, 1921–1934.
6. Shaw, P. H. Pathol Res Pract 1996, 192, 669–675.
7. Donehower, L. A.; Harvey, M.; Slagle, B. L.; McArthur, M. J.; Montgomery, C. A.; Butel Allenbradley, J. S. Nature 1992, 356, 215–221.
8. Jacks, T.; Remington, L.; Williams, B. O.; Schmitt, E. M.; Bronson, R. T.; Weinberg, R. A. Curr Biol 1994, 4, 1–7.
9. Harrison, C. A. P.; Peter, D.; Dobbie, A.; White, L.; Howie, S.; Salter, S.; Bird, D.; Wyllie, C. A. M. L. H. Oncogene 1994, 9, 603–609.
10. Okorokov, A. L.; Orlova, E. V. Curr Opin Struct Biol 2009, 19, 197–202.
11. Liu, D.; Song, H.; Xu, Y. Oncogene 2010, 29, 949–956.
12. Xu, Y. Oncogene 2008, 27, 3501–3507.
13. Tsang, W. P.; Ho, F. Y. F.; Fung, K. P.; Kong, S. K.; Kwok, T. T. Int J Cancer 2005, 114, 331–336.
14. Vaughan, C.; Singh, S.; Windle, B.; Yeudall, W.; Frum, R.; Grossman, S. R.; Deb, S. P.; Deb, S. Genes Cancer 2012, 3, 491–502.
15. Dent, P. Cancer Biol Ther 2013, 14, 879–880.
16. Xu, X. L. D. P. L. Y. Oncogene 2013, 29, 997–1003.
17. Wiech, M.; Olszewski, M. B.; Tracz-Gaszewska, Z.; Wawrzynow, B.; Zylicz, M.; Zylicz, A. PLoS One 2012, 7, e51426.
18. Stephen, C.; Lane, D. P. J Mol Biol 1992, 225, 577–583.
19. Gannon, J. V.; Greaves, R.; Iggo, R.; Lane, D. P. Embo J 1990, 9, 1595–1602.
20. Loh, S. N. Metallomics 2010, 2, 442–449.
21. Pavletich, N. P.; Chambers, K.; Pabo, C. O. Genes Dev 1993, 7, 2556–2564.
22. Cho, Y.; Gorina, S.; Jeffrey, P. D.; Pavletich, N. P. Science 1994, 265, 346–355.
23. Butler, J. S.; Loh, S. N. Protein Sci 2006, 15, 2457–2465.
24. Friedler, A.; Veprintsev, D. B.; Hansson, L. O.; Fersht, A. R. J Biol Chem 2003, 278, 24108–24112.
25. Lokshin, M.; Li, Y.; Gaiddon, C.; Prives, C. Nucleic Acids Res 2007, 35, 340–352.
26. Butler, J. S.; Loh, S. N. Biochemistry 2007, 46, 2630–2639.
27. Butler, J. S.; Loh, S. N. Biochemistry 2003, 42, 2396–2403.
28. Butler, J. S.; Loh, S. N. J Mol Biol 2005, 350, 906–918.
29. Linzer, D. I. H.; Levine, A. J. Cell 1979, 17, 43–52.
30. Zakut-houri, R.; Bienz-Tadmor, B.; Givol, D.; Oren, M. Embo J 1985, 4, 1251–1255.
31. Joerger, A. C.; Fersht, A. R. Annu Rev Biochem 2008, 77, 557–582.
32. Chen, Y.; Dey, R.; Chen, L. Structure 2010, 18, 246–256.
33. Selivanova, G. Semin Cancer Biol 2010, 20, 46–56.
34. Chen, F.; Wang, W.; El-Deiry, W. S. Biochem Pharmacol 2010, 80, 724–730.
35. Fu, T.; Min, H.; Xu, Y.; Chen, J.; Li, G. Int J Mol Sci 2012, 13, 9709–9740.
36. Wiman, K. G. Oncogene 2010, 29, 4245–4252.
37. Suad, O.; Rozenberg, H.; Brosh, R.; Diskin-Posner, Y.; Kessler, N.; Shimon, L. J. W.; Frolow, F.; Liran, A.; Rotter, V.; Shakked, Z. J Mol Biol 2009, 385, 249–265.
38. Eldar, A.; Rozenberg, H.; Diskin-Posner, Y.; Rohs, R.; Shakked, Z. Nucleic Acids Res 2013, 41, 8748–8759.
39. Boeckler, F. M.; Joerger, A. C.; Jaggi, G.; Rutherford, T. J.; Veprintsev, D. B.; Fersht, A. R. Proc Natl Acad Sci USA 2008, 105, 10360–10365.
40. Liu, X.; Wilcken, R.; Joerger, A. C.; Chuckowree, I. S.; Amin, J.; Spencer, J.; Fersht, A. R. Nucleic Acids Res 2013, 41, 6034–6044.
41. Yu, X.; Blanden, A. R.; Narayanan, S.; Jayakumar, L.; Lubin, D.; Augeri, D.; Kimball, S. D.; Loh, S. N.; Darren, R. Oncotarget 2014, 5, 8879–8892.
42. Lambert, J. M. R.; Gorzov, P.; Veprintsev, D. B.; Söderqvist, M.; Segerbäck, D.; Bergman, J.; Fersht, A. R.; Hainaut, P.; Wiman, K. G.; Bykov, V. J. N. Cancer Cell 2009, 15, 376–388.
43. Bykov, V. J. N.; Issaeva, N.; Shilov, A.; Hultcrantz, M.; Pugacheva, E.; Chumakov, P.; Bergman, J.; Wiman, K. G.; Selivanova, G. Nat Med 2002, 8, 282–288.
44. Saha, T.; Kar, R. K.; Sa, G. Prog Biophys Mol Biol 2014, 117, 250–263.
45. Wassman, C. D.; Baronio, R.; Demir, Ö.; Wallentine, B. D.; Chen, C. K.; Hall, L. V.; Salehi, F.; Lin, D. W.; Chung, B. P.; Hatfield, G. W.; Richard Chamberlin, A.; Luecke, H.; Lathrop, R. H.; Kaiser, P.; Amaro, R. E. Nat Commun 2013, 4, 1407.
46. Rueda, M.; Ferrer-Costa, C.; Meyer, T.; Pérez, A.; Camps, J.; Hospital, A.; Gelpí, J. L.; Orozco, M. Proc Natl Acad Sci USA 2007, 104, 796–801.
47. Blanden, A. R.; Yu, X.; Wolfe, A. J.; Gilleran, J. A.; Augeri, D. J.; O'Dell, R. S.; Olson, E. C.; Kimball, S. D.; Emge, T. J.; Movileanu, L.; Carpizo, D. R.; Loh, S. N. Mol Pharmacol 2015, 87, 825–831.
48. Aziz, M. H.; Shen, H.; Caki, C. G. Oncogene 2011, 30, 4678–4686.
49. Michaelis, M.; Rothweiler, F.; Agha, B.; Barth, S.; Voges, Y.; Löschmann, N.; von Deimling, A.; Breitling, R.; Wilhelm Doerr, H.; Rödel, F.; Speidel, D.; Cinatl, J. Cell Death Dis 2012, 3, e294.

50. Zeldovich, K. B.; Shakhnovich, E. Annu Rev Phys Chem 2008, 59, 105–127.
51. Pérez, A.; Marchán, I.; Svozil, D.; Sponer, J.; Cheatham, T. E.; Laughton, C.; Orozco, M. Biophys J 2007, 92, 3817–3829.
52. Case, D. A.; Darden, T. A.; Cheatham, I.; Simmerling, C. L.; Wang, J.; Duke, R. E.; Luo, R.; Walker, R. C.; Zhang, W.; Merz, K. M.; Roberts, B.; Hayik, S.; Roitberg, A.; Seabra, G.; Swails, J.; Götz, A. W.; Kolossváry, I.; Wong, K. F.; Paesani, F.; Vanicek, J.; Wolf, R. M.; Liu, J.; Wu, X.; Brozell, S. R.; Steinbrecher, T.; Gohlke, H.; Cai, Q.; Ye, X.; Wang, J.; Hsieh, M.-J.; Cui, G.; Roe, D. R.; Mathews, D. H.; Seetin, M. G.; Salomon-Ferrer, R.; Sagui, C.; Babin, V.; Luchko, T.; Gusarov, S.; Kovalenko, A.; Kollman, P. A. AMBER 12; University of California: San Francisco, 2012.
53. Homeyer, N.; Horn, A. H. C.; Lanig, H.; Sticht, H. J Mol Model 2006, 12, 281–289.
54. Pang, Y. P.; Xu, K.; El Yazal, J.; Prendergast, F. G. Protein Sci 2000, 9, 1857–1865.
55. Pang, Y. P. Proteins 2001, 45, 183–189.
56. Jorgensen, W. J Am Chem Soc 1981, 103, 335–340.
57. Roe, D. R.; Cheatham, I. I. I. T. E. J Chem Theory Comput 2013, 9, 3084–3095.
58. Humphrey, W.; Dalke, A.; Schulten, K. J Mol Graph 1996, 14, 33–38.
59. The PyMOL Molecular Graphics System, Version 1.7.4. Schrödinger, LLC.

Reviewing Editor: David Case